Egyptian Journal of Archaeological and Restoration Studies
An international peer-reviewed journal published bi-annually
www.ejars.sohag-univ.edu.eg

Original article

A STUDY OF THE DEGRADATION OF NATURAL ULTRAMARINE BLUE IN OIL PAINTINGS DUE TO THE INFLUENCE OF THE LOW SULFUR CONTENT S_3^- CHROMOPHORE IN THE COMPOSITION BY RAMAN ANALYSIS

Abo Taleb, Th.

Conservation dept., Faculty of Archaeology, Aswan Univ., Aswan, Egypt
E-mail address: dr.thanaa.ali@aswu.edu.eg

Article info.

Article history:
Received: 9-2-2022
Accepted: 20-11-2022
Doi: 10.21608/ejars.2022.276166

Keywords:
Ultramarine pigments
Blue chromophore S_3^-
Raman spectroscopy
IRFC
Discoloration

EJARS – Vol. 12 (2) – Dec. 2022: 205-215

Abstract:
The discoloration of natural ultramarine is related to the change in the molecular structure and crystal arrangements of the minerals due to the release of sulfur in acidic conditions. The acid breaks the Al-O bands and causes the cage to open permanently to allow access to the chromophore responsible for the color, S_3^- *released from the crystal structure and the loss of aluminum. Thus, a color change allows the release of the color-bearing radical anions. Thus, it is due to the natural ultramarine that has a stimulating effect on the dissolution of the binder (linseed oil), which leads to the appearance of a white dotted surface or heterogeneous white lines on the surface of the blue color or darkening dark gray more homogeneous. The study aims to study the mechanism of color change to grey whiteness in one of the oil paintings dating back to the late nineteenth century from the Gezira Museum in Cairo. It was carried out several examinations using stereo microscopy, polarized microscopy, spectroscopy photo by (VIS-UV-IR-IRFC), and analyses by color photometer, Raman and XRD methods, and related techniques (such as FTIR ART and SEM-EDX).*

1. Introduction

Archaeological evidence shows that the first appearance of lapis lazuli used in painting on wall paintings was in the sixth and seventh centuries in the cave temples of Bamiyan in Afghanistan and Europe [1]. It was used from the 14th century to the middle of the 15th century in decorative manuscripts and Italian paintings. It was dedicated to the robe of Christ and the Virgin in the late 16th and 17th centuries [2]. The discoloration of natural ultramarine blue on the surface of the oil paintings changes to a white dotted surface or inhomogeneous white stripes or darkens and turns dark gray, which is more homogeneous [3]. Ultramarine blue $Na_8Al_6Si_6O_{24}S_2$ contains sulfur in crystals, which causes the blue color [4]. The radical anion S_3^- is mainly responsible for the blue color. This sulfur radical anion is highly reactive but stable through the pigment structure. It is not affected by light, heat, or alkaline solutions but by acids. It is composed of an aluminum/silicon structure built of tetrahedral units AlO_4 and SiO_4 bonded with common oxygen [5]. The sodium cations act as a charge balancer [6]. The aluminum silicate mesh forms a framework of cube-octahedral cavities (also known as cages) capable of encapsulating atoms and small molecules in the cavities. It is the trapping and subsequent stabilization of sulfur radical anions (chromophores) specifically S_3^- and S_2^- [7] that play a role in the color of the pigment [8] at room temperature. They cannot escape

from the sodalite cage due to their size, resulting in color stability, but the cage is easily damaged by acids and alkalis exposure [9]. The ultramarine change is caused by many factors that are either additives, different ratios of $\mathbf{S_3^-}$ to $\mathbf{S_2^-}$, or a combination of both. The binding can deteriorate in the presence of moisture [10], or change color from mixing smalt blue [11], or due to the acid attack of the pigment by pollutants, biological metabolites, or even the acidity of the binder and the zeolite structure of the mineral that allows for ion exchange resulting from the hydrolysis of the oil medium and the formation of the metallic mineral soap and the metal carboxylation on the surface [12, 13]. Ultramarine can have a catalytic effect on the decomposition of the binder, as it contains sulfur-saturated zeolites [14,15]. Different analytical techniques were used to explain aspects of the degradation, such as energy-dispersive X-ray fluorescence (EDX), X-ray powder diffraction (XRD), and infrared of Raman. The value of peaks of S_3^- and S_2^- determines the color of ultramarine pigment, which indicates that it contains S fully reduced to form $\mathbf{S_3^-}$ (543 cm^{-1} peaks) and $\mathbf{S_2^-}$ groups (shoulder around 590 $cm^{-)}$. Therefore, the analysis of Raman spectra is very important to correlate it with the chromatometric [16]. Infrared (IR) spectroscopy has only been used to check the spectrum of the sodalite [17].

2. Materials and Methods

2.1. *Materials*

The study was carried out on an oil painting back to the late nineteenth century entitled “A Battle of War” from the Al-Jazeera Museum with a record number of 88, executed on a linen stand stretched on wood and applied on a white ground layer. It measures (80 cm wide×63 cm long), as shown in fig. (1). The painting depicts a war battle, and the artistic style of painting belongs to the Naturalistic’ painting style interested in studying the landscape. The painting is a scene with main elements, namely the sky and the weather. It has some soldiers riding horses. This landscape was classified according to the concept of the romantic school into the historical-heroic landscape that deals with heroic historical themes. It is one of the classic natural landscapes. The painting is unsigned. Its date of the painting refers to the late nineteenth century in the museum record. The painting suffers from some deterioration, especially fading, blue discoloration, loss of color layer, cracks, missing paint, and black spots.

Figure (1) Shows the painting from the front surface and some aspect of deterioration

2.2. *Methods*

An analytical examination study was conducted on two samples falling from the painting. Sample from the blue colored sky region on the upper right contained a two-color area (light-dark), and the other was a dark blue color in the dunes region on the bottom right. The varnish layer was removed from the surface of the samples before examinations and analyses.

2.2.1. Visual examination and photography

Photography was done in natural, oblique, and ultraviolet light because of being the most useful for examining the painting. The painting was placed in a dark room. The halogen light source must be placed at an angle of 45° on the surface of the paint at the corners of the painting. The light was transmitted onto the surface, exposing the topography of the painted surface. The photographs were done with a Canon® EOS camera and Canon EOS 5D Mark III.

2.2.2. Multispectral imaging

Imaging was done with near infrared (NIR), ultraviolet (UV), and false-color infrared"(IRFC) to study the surface and

damage. UV-induced imaging was carried out by lamps designed to emit in the UVA region with an emission of 365 nm using filters and UV lamps. Infrared-induced imaging was done with a FUJIFILM IS pro camera, with filters used to block visible light and transmit infrared Kodak Wratten #87 filters (cut at 740 nm). Moreover, Infrared False Color photography (IRFC) was done by digital rectifying VIS images. This technology depended on the overlay of two images: A digital image in daylight is overlaid with an infrared digital image. This type of image is called "false-color infrared" because the actual image is outside the spectral value of the infrared light. The wavelength of the infrared image is in the spectrum range of 780-900 nm; it allows for detecting and identifying pigments visually, such as distinguishing azurite blue and ultramarine. Moreover, it is useful for detecting retouchers. The IRFC does not provide conclusive results, but it aids in recognizing it as a valid tool for color identification besides analytical studies.

2.2.3. Spectrophotometer analysis

Colors were measured using a color photometer CM 2600 D by Konica with software spectra Magic NX, which is the most accurate data that can be found for studying color change [18]. These numerical values are characteristic of the color and content measurement compared between the blue area and the area that had a change to gray color in the visible region.

2.2.4. Optical and polarizing microscope

A sample was prepared for the cross-section by combining a sample of blue in CEM4000 resin and soften by sand-paper (1200-1500) to form the cross-section and examining under a stereo microscope attached with a Nikon digital 56 camera DMX 1200F and polarizing microscope (ECLIPSE LV100POL).

2.2.5. Scanning electron microscope attached to Energy-dispersive (SEM-EDX) and X-ray diffraction (XRD) analyses

SEM examination was used to study the structure of paintings, assess the state of damage, and analyze the color layer by EDX, making a map of the elements on the surface by EDX, in addition to the compound analysis by XRD to confirm the elements analysis.

2.2.6. FTIR analysis

FTIR Model Cary 630 FTIR spectrometer was used in the spectral range from 400 cm^{-1} to 4000 cm^{-1}, which is a useful technique for identifying chemical compounds, whether organic or inorganic [19].

2.2.7. Raman spectrometer

Raman spectroscopy was performed using Reni Shaw at 633 nm and 785 nm excitation sources [20]. It was coupled with a microscope. The spectral interpretation is highly dependent on a comparison with known reference materials. Raman is attached to the light microscope and was used to analyze two areas of colored surface damage: A blue area and a gray area on the same sample surface.

3. Results

3.1. *Surface examination*

Visual examination and photography with visible light and oblique light showed damage, and different color layers, indicating that the method used was *Alla Prima Painting Technique* in the area of green dunes and color changes from blue to gray in some parts of the sky. The examination showed white and black spots on the surface from the left side at the top of the painting and falling parts from the layer of the paint on the left side at the bottom, as shown in fig. (2-a-b). It also showed the darkening of the varnish layer. The oblique light showed an irregular surface, smears, white spots, efflorescence, gray calcifications, and a thickness of 1 mm on the surface, as shown in fig. (2-c).

Figure (2) Shows **a.** discoloration of the blue color, **b.** opacity and white dots, **c.** flaking

3.2. *Multispectral imaging*

Ultraviolet spectrophotometry, fig. (3-a) showed various damage, such as color change, unevenness of the surface, loss of color, torns and a small hole in canvas, The infrared imaging showed the flaking of the color layer, the opacity of the varnish layer, as shown in fig. (3-b). The imaging (IRFC) showed infrared rays, as shown in figs. (3-c & d). Ultramarine blue appears bright because it reflects infrared rays, while the azurite blue appears drake because it absorbs infrared rays.

Figure (3) Shows the layers painted by different spectral bands using a modified Nikon digital camera; **a.** ultraviolet fluorescence (UVF), **b.** infrared (IR) **c.** & **d.** infrared false color (IRFC).

3.3. *Spectrophotometer analysis*

The coulometer analysis showed the values of blue color L* = 24, a*= 20, b* = -58 and the values of gray color L* = 26, a* = 22, b* = - 06. It resulted in chromatic differences, where,

$$\Delta E = \sqrt{\Delta L* + \Delta a* + \Delta b*} = \Delta E = 3.4$$

The difference in the degrees of the blue color was proved through the different color values, as the change was the values of L*, b*, and a*. The values of the whiteness L* (Lightness) increased from 22 to 26, the values of a* (red/green) increased from 20 to 22, and the b* values (blue/yellow) decreased from -58 to -60.

3.4. *Optical and polarizing microscope investigation*

The examined cross-section by stereo microscopy indicated that the layers of the paintings consist of three layers. The 1st layer is degraded canvas, the 2nd layer is ground calcium carbonate (determined by FTIR), and the 3rd layer is ultramarine blue degraded paint. The examination indicated the appearance of very thin white dots around the grains of the colored substance, and some other areas had different stages of color change, erosion of the bonding material between the color atoms, and loss of color saturation, fig. (4-a). The examined thin-section by polarizing microscopy indicated that canvas was linen fibers' cylindrical bundles as the fibers are straight and show transverse breaks, as well as The fibers deteriorated, and the paint layer ultramarine blue deteriorated with the discoloration to grey, fig. (4-b). The examination of the sample by stereomicroscope magnification 20-X, fig. (5,a-b-c) indicated the severe weakness of the canvas and the damage to the color layer, the change of the blue color in the sky to gray, as well as the swelling of the color layer and the for-mation of holes which lead to rise between the layers of colors and their cracks.

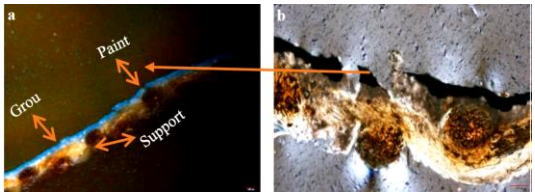

Figure (4) Shows a cross-section of deterioration features; **a.** structure layers using SM, **b.** paintings layers using PM.

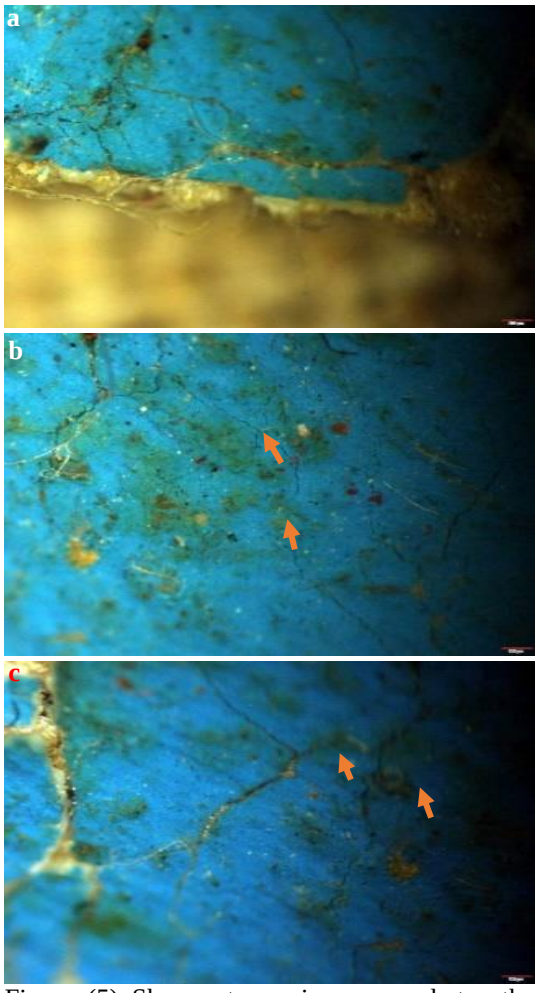

Figure (5) Shows stereomicroscope photos the blue sample color; **a.** cracks, **b.** blue color changing to gray and white dots, **c.** flaking and color fall off.

3.5. *EDX-SEM and XRD*

SEM-EDX analysis, element map, and cross-section, figs. (6-a & b), indicated that the light blue color sample contained some elements, such as (Na, Al, Si, and S) and others. The color was composed of silica (7.03%), aluminum (8.79%), calcium (0.60%), sodium (7.45%), sulfur (5.80%), carbon (28.14%), and oxygen (42.18%), fig. (6-a). The analysis of the dark blue sample indicated that it contained silica (1.46%), aluminum (1.11%), calcium (2.77%), sodium (1.47%), sulfur (3.52%), carbon (25.54%), oxygen (56. 68%), copper (5.03%), titanium (0.3%), iron (1.01%), and magnesium (0.71%), fig. (6-b).

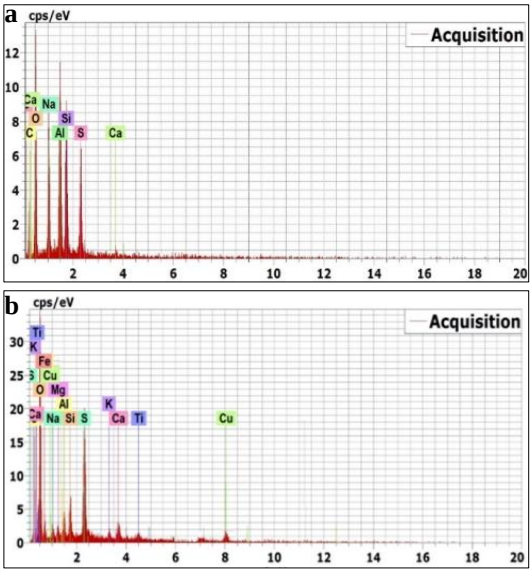

Figure (6) Shows EDX analytical results; **a.** light blue sample, **b.** bluish dark sample from the sky area.

SEM examination showed discoloration in blue color (dark area and white circular area) and surface roughness, as shown in figs. (7-a & b). The element map in the ultramarine sample by EDX indicated that the element with atomic number > 11 as (Na, Al, Si, S), fig. (8).

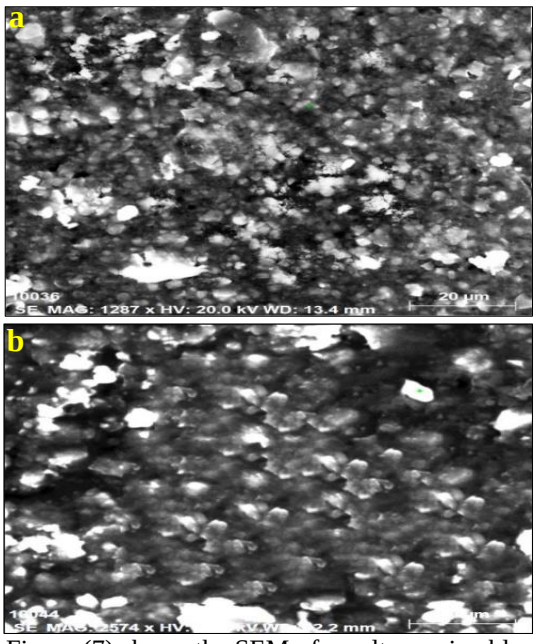

Figure (7) shows the SEM of an ultramarine blue sample in the sky area colored; **a.** surface roughness, **b.** dark area and white circular area

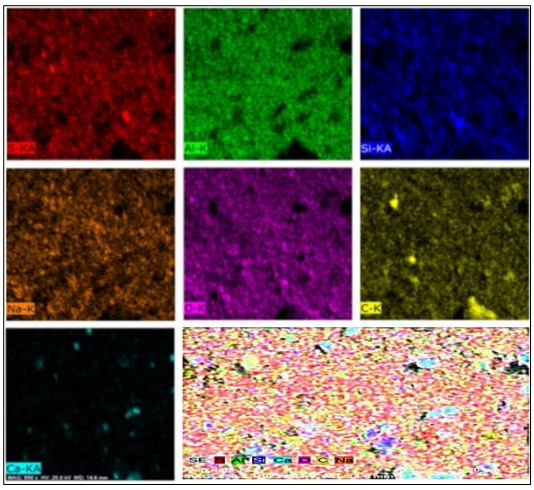

Figure (8) Shows EDX elemental map of blue color

XRD analysis, as shown in fig. (9-a), showed that the light blue color was ultramarine (13.7%), a cubic blue mineral and silica dioxide by (18.6%), carbon (23%), and the organic compound naphthalene carboxylic acid $C_{10}H_7CO_2H$ (44.8%) that is one of the two simultaneous monocarboxylic acids of naphthalene resulting from the degradation of the oily medium. XRD, fig. (9-b) showed that the dark blue color sample was made up of mixing ultramarine blue (23.9%) with azurite blue (16.6%), as well as calcite (27%) and gypsum (21.4%).

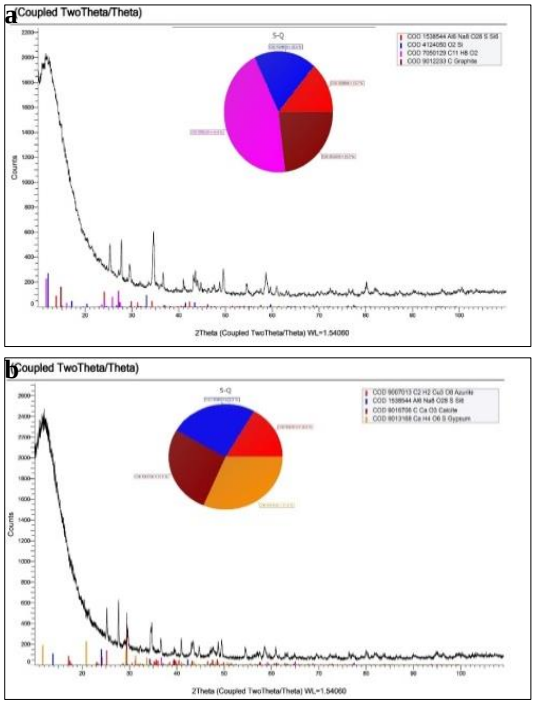

Figure (9) Shows X-ray diffraction patterns of **a.** Ultramarine, **b.** Azurite blue samples

3.6. *Fourier transform infrared spectral analysis (FTIR)*

The results of the FTIR of the ultramarine sample, fig. (10-a) indicated the presence of the S_3^- ion, which is primarily responsible for the blue color at the wavelength 580 cm^{-1} and the presence of ultramarine blue. For the existence of the sodalite structure in the Si-0 expansion region of the aluminosilicate matrix, at a wavelength of 1010 cm^{-1} and wavelengths of 1150 cm^{-1}, 1100 $cm^{-1,}$ and 1370 cm^{-1}, the analysis showed the presence of Al-O and Si-O groups of aluminum silicates $[(Al_6Si_6)\ O_{24}]$ at wavelengths of 750 cm^{-1} and 650 cm^{-1}, calcite ($CaCo_3$) at the wavelengths of 706. 879 cm^{-1} and 1450 cm^{-1}, linseed oil at the wavelengths of 2918 cm^{-1},2850 cm^{-1} and 1735 cm^{-1}, and water sulfate gypsum due to the presence of the (OH) group at the wavelengths of 1610 cm^{-1} and 3410 cm^{-1}. The analysis of the dark blue, fig. (10-b), indicated the presence of azurite $Cu_2CO_3(OH)_2$ due to the group CO_3^{2-} stretching at the wavelengths of 1442.12 cm^{-1} and 2500.15 cm^{-1} and the silica group (Si–O–Al) at the wavelengths of 1032.68 cm^{-1} and 464.72 cm^{-1}. The blue spectra of azurite based on copper showed an absorption band at the wavelengths of 1543.21cm^{-1}, 1735.12 cm^{-1}, and 1424.12 cm^{-1}, the ultramarine blue absorption group (Al-O and Si-O) at the wavelengths of 1032.68 cm^{-1} and 668.42 cm^{-1}, and the ultramarine blue active group responsible for the blue color carrier S_3^- at a wavelength of 598.79 cm^{-1}. The analysis showed the active group $(SO_4)^{-2}$ for calcium salts at the wavelengths of 2010, 2114 cm^{-1}, 2031cm^{-1}, 2023 cm^{-1}, 1646.82 cm^{-1}, 1107.79 cm^{-1}, 1032.68 cm^{-1}, and 668.42 cm^{-1}. The spectrum appeared at the absorption peak of the Al–OH group at a wavelength of 2211.12 cm^{-1} [21]. The analysis indicated that the varnish was mastic for the presence of an OH absorption group at a wavelength of 3565.65 cm^{-1}, an absorption group υ (CH_3) at the wavelengths of 2973.11 cm^{-1} and 2870.33 cm^{-1}, and an absorption group υ (CH_2) at a

wavelength of 2870.33 cm^{-1}. It could distinguish resins by the usually weak and broad groups, such as the OH carboxyl absorption groups at a wavelength of 2500.15 cm^{-1}, the C=O str absorption group at the wavelengths of 1735.12 cm^{-1} and 1646.82 cm^{-1}, the CH bend absorption group at the wavelengths of 1424.12 cm^{-1} and 1395 .05 cm^{-1}, the CH str absorption group at a wavelength of 2973.11 cm^{-1}, and the C=O str absorption group at a wavelength of 1275.68 cm^{-1} [22]. It also showed the calcium carbonate group at the wavelengths of 1543.21 cm^{-1}, 1424.12 cm^{-1}, and 2500.15 cm^{-1},

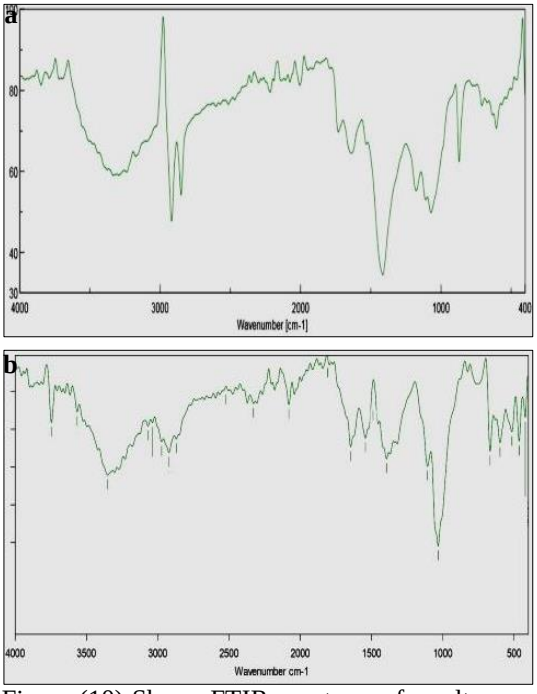

Figure (10) Shows FTIR spectrum of **a.** ultramarine, **b.** the Azurite blue absorption bands

3.7. *Raman analysis*

The analysis of Raman spectra used to study the change in the radical anion responsible for the blue color - in two regions, one of which was (*blue*) and the other; its color changed from blue to (*grey*), and the comparison between them, fig. (11-a & b). Raman analysis of the gray color region showed the stretching vibrations bands S_3^- (585 cm^{-1}) and S_2^- (549 cm^{-1}), as shown in fig. (11-c) (red chart). As well as analysis of the blue color region showed the stretching vibrations bands S_3^- blue chromophore (590cm^{-1}) and S_2^- yellow chromophore (555 cm^{-1}) (blue chart). The comparison of the spectra illustrated a difference in the values of S_2^- and S_3^- in both regions, blue and gray, as a result of damage as shown fig. (11-c), which, showed a clear decrease in the signal of S_2^- (555 cm^{-1}) to (549) cm^{-1} and a decrease in S_3^- (590 cm^{-1}) to (585 cm^{-1}). A difference is seen between the spectra from the blue area and the white. Accordingly, a decrease in the spectra of chromophore was observed in the decomposing color (gray color).

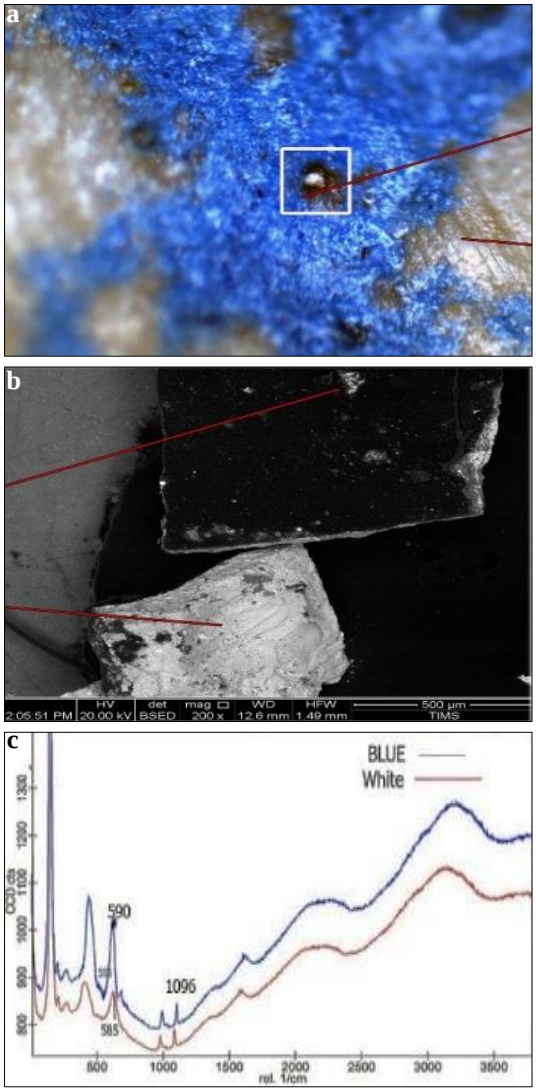

Figure (11) Shows **a.** Raman optical image of blue area contains both *blue* and *white* (degraded paint) which, is heterogeneous blue particles containing a number of gray particles, **b.** SEM photomicrograph of the same sample, **c.** Raman spectra taken from the blue and gray areas.

4. Discussion

Examining the surface by slope light and stereo microscope showed that the ultramarine blue changed to gray with white lines intersecting with the surface. There were cracks across the surface of the paint, which resulted from the hydrolysis of oil due to exposure to unsuitable environmental factors, such as changes in RH, high AT, aging oil medium, or light [23]. The XRD analysis indicated that the blue sample of natural ultramarine was confirmed by EDX analysis, and ultramarine ($Na_8Al_6Si_6O_{24}S_2$) contained the radical anion S^-_3 responsible for the blue color of the dye. The radical anions could move from the crystal structure of the color through the effect of acids resulting from air pollutants [24], such as sulfur dioxide (SO_2), and the exposure to alkalis and light, causing a color change [25]. The presence of the organic compound naphthalene carboxylic acid, an organic compound resulting from the deterioration of the oily medium from the effect of unsuitable environmental conditions, resulted in the color change [26]. The presence of gypsum suggested that it was possible that the $\boldsymbol{S_3^-}$ radical groups were liberated from the crystal structure and reacted with moisture to form sulfuric acid, which reacted with the decomposed ground layer to form gypsum. [27]. The analysis of the dark blue sample indicated that the artist used the mixing ultramarine blue in a large ratio and azurite in a lesser ratio to obtain a darker color tone. The FTIR analysis proved the presence of Al-O and Si-O groups probably due to the effect of acids breaking Al-O bonds and a discrepancy in the coordination of aluminum, causing the destruction of the structure, [28] which in turn led to the release of the chromophore, the loss of color, and the appearance of an additional aluminum frame that led to the permanent opening of the cage and the release of chromophores and to allow access to the chromophores, and thus a change in the color [29]. The analysis indicated that the color change might be due to containing alkaline silicates (potassium and sodium) [30] depleted from the crystal structure [31] and migrating to the surface, leading to the color change. The Raman analysis of the two colors (blue-grey) on the same sample confirmed that the sample contained $\boldsymbol{S_3^-}$ (blue) at the spectral of 590 cm^{-1} and belonging to the $\boldsymbol{S_3^-}$ ion where the $\boldsymbol{S_3^-}$ radical anion was mainly responsible for the blue color [17]. Comparing the two regions in the sample illustrated that radical anion $\boldsymbol{S_3^-}$ decreased from 590 cm^{-1} in the blue region to 585 cm^{-1} in the gray region. Accordingly, a decrease in the spectral of chromophore $\boldsymbol{S_3^-}$ was in the decomposing paint, which had a color change to gray. The colorimetric measurements of ultramarine blue showed the increase in the lightness (L*) related to the decrease in pigment saturation. Thus, we found that lightness (L*) increased in the gray region. In contrast, it decreased lightness in the blue region, indicating that the blue color, $\boldsymbol{S_3^-}$, mostly responsible for saturation and, therefore, for color intensity. Accordingly, the lightness (L*) of the pigments decreased with the increase in the concentration of chromophore $\boldsymbol{S_3^-}$, so the saturation of the colors increased and vice versa [17]. The analysis and examination of the mechanism of color change could be summarized according to the equations: ***)** Formation of acid in the gas phase; Damage could be caused by chemical reactions between wet dust and gases or by harmful compounds in deposited particles. It formed acidic compounds in the presence of moisture to give sulfuric acid, as noted in the next equation:

$S+O_2 \rightarrow SO_2$ / $SO_2 + 1.5\ O_2 \rightarrow SO_3$ / $H_2O + SO_3 \rightarrow H_2SO_4$.

***)** Dilute acids (HCl, HNO_3, and H_2SO_4) quickly destroyed ultra-marine blue and produced hydrogen sulfide, resulting in blackening. Cage opening mechanism: The acids broke the aluminosilicate network (β-cage), and the Al-O bonds broke and caused the cage to open constantly to allow access to and release of the chromophore and the loss of aluminum; thus, a

discoloration occurred, as in could be noted in the next equations:

$$Na_8\,[AL_6Si_6\,O_{24}(S_3^-S_2^-\,)+\,H_2SO_4+H_2O(g)$$

$$Na_8\,[AL_6Si_6\,O_{24}\left(S_3^-S_2^-\right)+\,AL(OH)_3+\,(g))$$

Chromophore Reactions: Ultramarine blue contained S_3^- (blue) and S_2^- (yellow) chromophores, and the radical anion S_3^- was primarily responsible for the blue color. The chromophores released and reacted. The oxidation of the S-rich particles to H_2so_4 could cause the discoloration of ultramarine blue and deterioration of the paint [32], as in could be noted in the next equations:

$$2S_3^- + H_2SO_4\,(aq) + 2O_2 + 2H_2O\,(g) \rightarrow SO_4^{2-} + 3H_2S\ (g) + 3SO_2\ (g)\ /\ S_3^- + 2s_3^- + H_2SO_4\,(aq) + 1.5O_2 + 2H_2O\,(g) \rightarrow SO_3^{2-} + 3H_2S\ (g) + 3SO_2(g)$$

5. Conclusion

Upon the above mentioned data Ultramarine blue ($Na_8Al_6Si_6O_{24}S_2$) contains the radical anion S-3, which is responsible for the blue color. This material may have been changed as a direct result of several deterioration factors, such as damage that occur due to chemical reactions between wet dust with some dominated types of gases, and acidic compounds, especially with the presence of other types of moisture, particularly, with Al ion. This mechanism that have led to the effect of the cage and the release of the chromophore responsible for the color. Moreover, Raman analysis had showed the severe damage by comparing two regions showing a clear decrease in the chromophore S-3 signal intensity in the white lines on the coating surface, compared to the blue regions. This result had been confirmed by other analytical techniques such as, EDX, XRD FTIR and the elemental mapping.

Acknowledgments

The authors would like to thank Prof. Badawy Ahmed Enis, Molecular spectroscopy unit, NRC, Cairo for his great helping in analyzing and interpreting Raman analysis, and Prof. Dr. Abo-EL Hamad Hassan, Analytical Chemistry dept., Faculty of Science, Aswan Univ. for reviewing FTIR, and XRD analytical results.

Reference

[1] Plesters, J. (1986). *Ultramarine blue, natural and artificial artists' pigments: A handbook of their history and characteristics*, Vol. (2), Oxford Univ. Press, Oxford.

[2] Harley, R. (1982). *Artists' pigments, c. 1600-1835: A study in English documentary sources*, Archetype Pub., London.

[3] Hommes, E. (2004). *Changing pictures: Discolouration in 15th-17th century oil paintings*, Archetype Pub., London.

[4] Zorba, T., Pavlidou, E., Stanojlovic, M., et al. (2006). Technique and palette of XIIIth century painting in the mon-astery of Mileseva. *Applied Physics A*, Vol. 83, (4), pp. 719-725.

[5] Bicchieri, M., Nardone, M., Russo, P., et al. (2001). Characterization of azurite and lazurite-based pigments by laser-induced breakdown spectroscopy and micro-Raman spectroscopy, *Spectrochimica Acta Part B: Atomic Spectroscopy*, Vol. 56 (6), pp. 915-922.

[6] Fleet, M., Liu, X., Harmer-Bassell, S., et al. (2005). Sulfur K-edge XANES spectroscopy: Chemical state and content of sulfur in silicate glasses, *The Canadian Mineralogist*, Vol. 43 (5), pp. 1605-1618.

[7] Reinen, D., & Lindner, G. (1999). The nature of the chalcogen colour centres in ultramarine-type solids, *Chemical Society Reviews*, Vol. 28 (2), pp. 75-84.

[8] Miliani, C., Daveri, A., Brunetti, B., et al. (2008). CO_2 entrapment in natural ultramarine blue, *Chemical Physics Letters*, Vol. 466 (4-6), pp.148-151.

[9] Hamerton, I., Tedaldi, L. & Eastaugh, N., (2013). A systematic examination of colour development in synthetic ultramarine according to historical methods. *Plos One*, Vol. 8 (2), doi: org/10.1371/journal.pone.0050364

[10] Bacci, M., Magrini, D., Picollo, M., et al. (2009). A study of the blue colors used by Telemaco Signorini (1835-1901), *J. of Cultural Heritage*, Vo. 10 (2), pp. 275-280.

[11] Wyld, M., Mills, J. & Plesters, J. (1980). Some observations on blanching (with special reference to the paintings of Claude), *National Gallery Technical Bulletin*, Vol. 4, pp. 49-63.

[12] Leo, R. (2000). Minerals and the visual arts, *J. of Geoscience Education*, Vol. 48 (3), pp. 317-320.

[13] Bacci, M., Magrini, D., Picollo, M., et al. (2009). A study of the blue colors used by Telemaco Signorini (1835-1901), *J. of Cultural Heritage*, Vol. 10 (2), pp. 275-280.

[14] Dudzik, Z. & Preston, K. (1968). Paramagnetism and catalytic activity of sulfur-impregnated zeolites, *J. of Colloid and Interface Science*, Vol. 26 (3), pp. 374-378.

[15] Gambardella, A., Cotte, M., de Nolf, W., et al. (2020). Sulfur K-edge micro- and full-field XANES identify marker for preparation method of ultramarine pigment from lapis lazuli in historical paints, *Science Advances*, Vol. 6 (18), doi: 10.1126/sciadv.aay 8782..

[16] Ledé, B., Demortier, A. Gobeltz-Hautecœur, N. et al. (2007). Observation of the ν3 Raman band of S_3^- inserted into sodalite cages, *J. of Raman Spectroscopy*, Vol. 38, (11), pp. 1461-1468.

[17] Gobeltz, N., Demortier, A. Lelieur, J., et al. (1998). Correlation between EPR, Raman and colorimetric characteristics of the blue ultramarine pigments, *J. of the Chemical Society, Faraday Transactions*, Vol. 94, (5), pp. 677-681.

[18] Susan, D., Sorensen, N., Michael, J., et al. (2014). Investigation of steel lug nut failures with brittle fracture characteristics. *Microscopy and Microanalysis*, Vol. 20 (S3), pp. 1862-1863.

[19] Van der Weerd, J., van Loon, A. & Boon, J. (2013). FTIR studies of the effects of pigments on the aging of oil. *Studies in Conservation*, Vol. 50 (1), pp. 3-22.

[20] Holzer, W., Murphy, W. & Bernstein, H. (1969). Raman spectra of negative molecular ions doped in alkali halide crystals. *J. of Molecular Spectroscopy*, Vol. 32 (1), pp. 13-23.

[21] Berrie, B. (2007). *Artists' pigments: A handbook of their history and characteristics*, Vol. 4, National Gallery of Art, Washington.

[22] Derrick, M., Stulik, D. & Landry, J. (1999). *Infrared spectroscopy in conservation science*, Paul Getty Trust Los Angeles, USA

[23] Monico, L., Janssens, K., Cotte, M., et al. (2016). Chromium speciation methods and infrared spectroscopy for studying the chemical reactivity of lead chromate-based pigments in oil medium, *Microchemical J.*, Vol. 124, pp. 272-282.

[24] Reinen, D. & Lindner, G. (1999). The nature of the chalcogen colour centres in ultramarine-type solids, *Chemical Society Reviews*, Vol. 28 (2), pp. 75-84.

[25] Hackney, S. (1984). The distribution of gaseous air pollution within museums, *Studies in Conservation*, Vol. 29 (3), pp. 105-116.

[26] Chiavari, G., Fabbri, D. & Prati, S. (2002). Characterisation of natural resins by pyrolysis—Silylation, *Chromatographic*, Vol. 55 (9), pp. 611-616.

[27] Pozo-Antonio, J., Rivas, T., Dionísio, A., et al. (2020). Effect of an SO_2 rich atmosphere on tempera paint mock-ups. Part 1: accelerated aging of smalt and lapis lazuli-based paints, *Minerals*, Vol. 10 (5), doi: org/10.3390/min100 50427

[28] Hendrickx, R., Desmarais, G., Weder, M., et al. (2016). Moisture uptake and permeability of canvas paintings

and their components, *J. of Cultural Heritage*, Vol. 19, pp. 445-453.

[29] Janssens, K., Van der Snickt, G., Vanmeert, F., et al. (2017). Non invasive and non-destructive examination of artistic pigments, paints, and paintings by means of X-ray methods, in: Mazzeo, R. (ed.) *Analytical Chemistry for Cultural Heritage*, springer, Switzerland, pp. 77-128.

[30] Robinet, L., Spring, M., Pagès Camagna, S., et al. (2011). Investigation of the discoloration of smalt pigment in historic paintings by micro-X-ray absorption spectroscopy at the Co K-edge, *Analytical Chemistry*, Vol. 83 (13), pp. 5145-5152.

[31] McKeown, N., Bishop, J., Cuadros, J., et al. (2011). Interpretation of reflectance spectra of clay mineral-silica mixtures: Implications for Martian clay mineralogy at Mawrth Vallis, *Clays and Clay Minerals*, Vol. 59 (4), pp. 400-415.

[32] Del Federico, E., Shöfberger, W., Schelvis, J., et al. (2006). Insight into framework destruction in ultramarine pigments, *Inorganic Chemistry*, Vol. 45 (3), pp. 1270-1276.